Human Molecular Genetics, 2011, Vol. 20, No. 13 **2560–2570**
doi:10.1093/hmg/ddr155
Advance Access published on April 14, 2011

The Usher 1B protein, MYO7A, is required for normal localization and function of the visual retinoid cycle enzyme, RPE65

Vanda S. Lopes[1,2,3,4], Daniel Gibbs[3,†], Richard T. Libby[5,‡], Tomas S. Aleman[6], Darcy L. Welch[1], Concepción Lillo[3,§], Samuel G. Jacobson[6], Roxana A. Radu[1], Karen P. Steel[5,7] and David S. Williams[1,2,3,*]

[1]Jules Stein Eye Institute and [2]Department of Neurobiology, UCLA School of Medicine, 200 Stein Plaza, Los Angeles, CA 90095, USA, [3]Department of Pharmacology and Department of Neurosciences, UCSD School of Medicine, La Jolla, CA 92093, USA, [4]Centre of Ophthalmology, IBILI, University of Coimbra, 3048 Coimbra, Portugal, [5]MRC Institute of Hearing Research, University Park, Nottingham NG7 2RD, UK, [6]Scheie Eye Institute, Department of Ophthalmology, University of Pennsylvania, Philadelphia, PA 19104, USA and [7]The Wellcome Trust Sanger Institute, Hinxton, Cambridge, CB10 1SA, UK

Received February 7, 2011; Revised and Accepted April 7, 2011

Mutations in the *MYO7A* gene cause a deaf-blindness disorder, known as Usher syndrome 1B. In the retina, the majority of MYO7A is in the retinal pigmented epithelium (RPE), where many of the reactions of the visual retinoid cycle take place. We have observed that the retinas of *Myo7a*-mutant mice are resistant to acute light damage. In exploring the basis of this resistance, we found that *Myo7a*-mutant mice have lower levels of RPE65, the RPE isomerase that has a key role in the retinoid cycle. We show for the first time that RPE65 normally undergoes a light-dependent translocation to become more concentrated in the central region of the RPE cells. This translocation requires MYO7A, so that, in *Myo7a*-mutant mice, RPE65 is partly mislocalized in the light. RPE65 is degraded more quickly in *Myo7a*-mutant mice, perhaps due to its mislocalization, providing a plausible explanation for its lower levels. Following a 50–60% photobleach, *Myo7a*-mutant retinas exhibited increased all-*trans*-retinyl ester levels during the initial stages of dark recovery, consistent with a deficiency in RPE65 activity. Lastly, MYO7A and RPE65 were co-immunoprecipitated from RPE cell lysate by antibodies against either of the proteins, and the two proteins were partly colocalized, suggesting a direct or indirect interaction. Together, the results support a role for MYO7A in the translocation of RPE65, illustrating the involvement of a molecular motor in the spatiotemporal organization of the retinoid cycle in vision.

INTRODUCTION

Usher syndrome is a recessively inherited disorder of combined deafness and blindness. In Usher syndrome type 1, defects in the cochlear hair cells result in congenital, profound deafness and abnormalities in the retina lead to progressive degeneration of the photoreceptor cells after development. Mutations in the *MYO7A* gene cause Usher syndrome type 1B (1). Shaker1 mice have loss-of-function mutations in the orthologous gene, *Myo7a*, and thus serve as a model of Usher 1B (2).

MYO7A is an unconventional myosin motor protein (3,4), expressed both in retinal photoreceptors and the retinal pigmented epithelium (RPE) (5,6). Studies of shaker1 mice have demonstrated that MYO7A has important functions in

*To whom correspondence should be addressed. Email: dswilliams@ucla.edu
†Present address: The Salk Institute for Biological Studies, La Jolla, CA 92037, USA.
‡Present address: University of Rochester Eye Institute, Rochester, NY 14642, USA.
§Present address: Instituto de Neurociencias de Castilla y León, Salamanca, Spain.

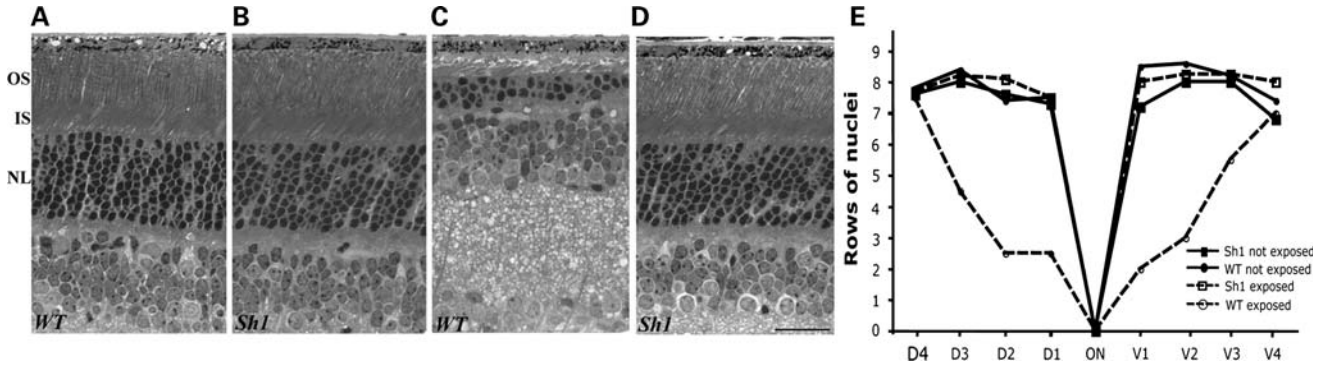

Figure 1. Shaker1 retinas are resistant to light damage. Light micrograph sections of retinas in the region located 0.5 mm dorsal to the optic nerve (ON) demonstrate the thickness of the photoreceptor cell nuclear layer in WT (**A** and **C**) and shaker1 (**B** and **D**) mice exposed to regular (A and B) or damaging (C and D) light. All animals were reared under the normal light/dark cycle. All images are of the same magnification; scale bar = 50 μm. OS, outer segment layer; IS, inner segment layer; NL, photoreceptor nuclear layer. (**E**) Quantification of photoreceptor cell nuclei at 0.5 mm intervals from the optic nerve head in dorso-ventral sections of retinas of the animals described in (A)–(D). Each value corresponds to the mean obtained from retinas of three different animals (SEM <0.55 in all cases).

both cell types. In the photoreceptors, MYO7A is required for the normal transport of opsin through the ciliary plasma membrane to the outer segment (7), and, in the RPE, it functions in the movement of melanosomes and phagosomes (8–10). However, as with most of the mouse models of the other Usher 1 genes, shaker1 mice have been found not to undergo retinal degeneration, at least under standard vivarium conditions (11).

We began the present study by attempting to see if shaker1 retinas could be induced to degenerate, if stressed. We tested whether shaker1 mice were more susceptible to retinal degeneration that occurs in response to high-light exposure (12), as already shown for several other animal models of retinal degeneration (13–17). To our surprise, we found that retinas of shaker1 mice were more *resistant* to light damage than retinas of wild-type (WT) mice on the same genetic background.

Following the absorption of a photon of light, rhodopsin becomes bleached. It is then regenerated following a series of reactions, known as the visual retinoid cycle, that involves the formation of 11-*cis* retinal, the light-sensitive ligand that binds to opsin (18–21). Defects in rhodopsin regeneration can afford protection against light damage (22). Hence, our finding on resistance to light damage in shaker1 mice led us to study the requirement for MYO7A in the retinoid cycle. Our study focused on RPE65, an enzyme that catalyzes the conversion of all-*trans*-retinyl esters to 11-*cis* retinol, a key isomerization step in the retinoid cycle (23–25). We found that RPE65 translocates within the RPE in response to light. We report evidence that MYO7A functions in this translocation, and is thus an important element in the spatiotemporal regulation of the visual retinoid cycle.

RESULTS

Retinal degeneration in response to short-term high-light exposure

Shaker1 mice carrying the *Myo7a*^{4626SB} allele on a mixed genetic background (see Materials and Methods) were used in an acute light damage experiment. They were determined by polymerase chain reaction (PCR) to be homozygous for the normal Leu450 allele of RPE65. Light microscopy of retinas from animals kept for 10 days after a 2 h exposure to 15 000 lux showed a significant loss of photoreceptor cells in WT mice (Fig. 1A and C). From a quantitative analysis of photoreceptor cells along the entire dorso-ventral axis, it is clear that the central photoreceptors were especially affected (Fig. 1E). In contrast, high-light-exposed shaker1 retinas were comparable with unexposed retinas (Fig. 1B, D, E). Electroretinogram (ERG) measurements were consistent with the light microscopy. Amplitudes of the a-wave (the photoreceptor component of the ERG) were reduced by ∼50% in exposed WT retinas, whereas those of shaker1 (MYO7A null) retinas were unaffected by the high-light exposure.

This experiment was repeated with shaker1mice on a C57BL6 genetic background. The Met450 variant of the RPE65 protein is expressed in the C57BL6 genetic background, and is present at significantly lower levels than Leu450 RPE65 (26,27). In this case, neither the control nor mutant mice showed any damage to a 2 hr exposure to light of 15 000 lux.

Cellular amounts of visual cycle proteins

Because of the resistance of shaker1 retinas to light damage, and that defects in rhodopsin regeneration have been shown to afford protection against light damage (22), we tested whether the loss of MYO7A affects the cellular amounts of proteins involved in the visual cycle. Western blot analysis showed that the level of RPE65 was reduced in shaker1 retinas (Fig. 2A and B). However, the levels of other RPE proteins, such as lecithin:retinol acyl transferase (LRAT), cellular retinaldehyde-binding protein (CRALBP) and an RPE intracellular retinal GPCR (RGR), were not appreciably different. RPE65 levels in retinas obtained from mice during the afternoon (i.e. light-adapted (LA) for >6 h on their regular light cycle) were reduced by 30–50% in the absence of MYO7A. Interestingly, the level of RPE65 in heterozygote (*+/sh1*) retinas was in between the levels of WT and shaker1 retinas (Supplementary Material, Fig. S1).

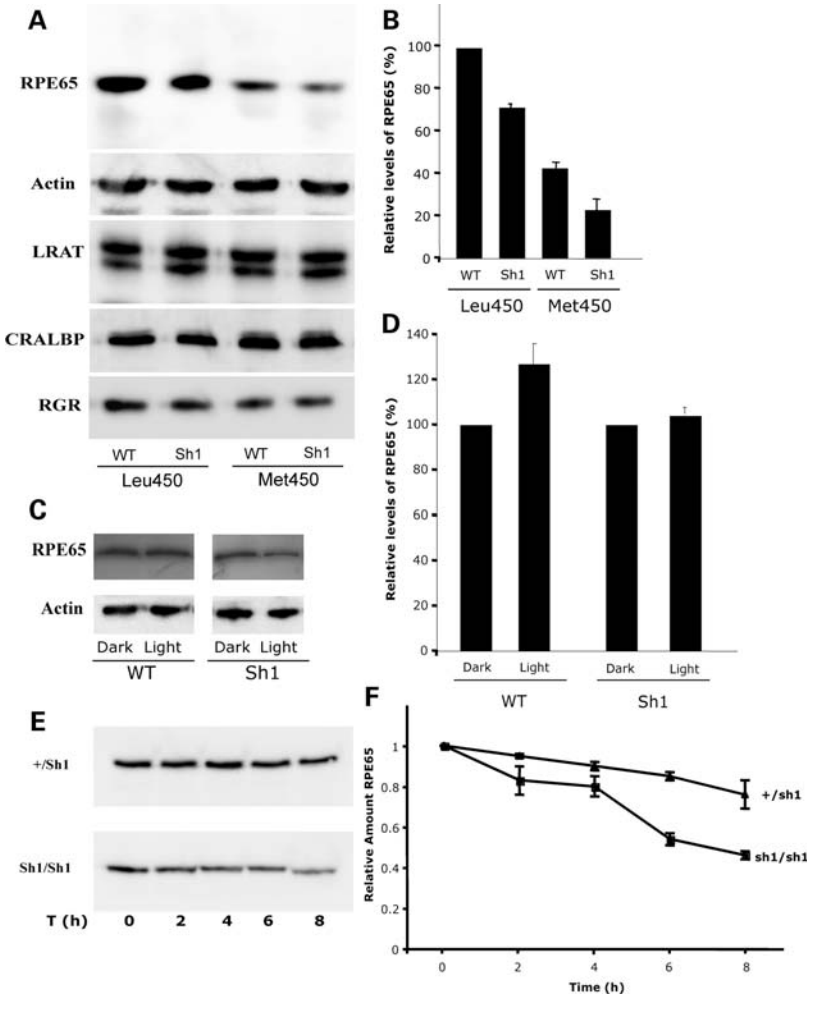

Figure 2. Levels of visual cycle proteins. (**A**) Ten micograms of WT and Sh1 eyecups, expressing the Leu450 or Met450 RPE65 variant, were probed by western blot for several visual cycle proteins. Actin was used as loading control. (**B**) Bar graph showing the relative percent of RPE65, measured from western blots, such as that shown in (A), by densitometry. Error bars represent $\pm$ SEM, where $n \geq 3$. Sh1 have reduced levels of RPE65 ($\sim$30% less; $P = 0.002$), independent of the RPE65 variant expressed in the RPE. (**C**) Western blotting analysis of dark-adapted (DA) (16 h) and LA (16 h dark + 2 h light) eyecups of WT and Sh1 mice. Actin was used as loading control. (**D**) Bar graph indicating the relative amount of RPE65 determined by densitometry ($n = 4$, error bars indicate SEM; probability of no significant difference between WT light and dark = 0.005). (**E**) Western blot of RPE65 in shaker1 (sh1/sh1) and heterozygous eyecups incubated for different lengths of time with CHX to inhibit protein synthesis. (**F**) Graph of relative amount of RPE65 with respect to length of time with CHX, showing accumulated data determined by densitometry of western blots from different experiments; error bars indicate SEM.

The relative reduction in RPE65 was irrespective of genetic background, and of whether or not that background carries the normal Leu450 allele of RPE65 or the Met450 variant. In shaker1 mice on the C57BL6 background, the Met450 variant is reduced further below than that in WT C57BL6 mice (Fig. 2A and B).

In further analysis, we found that the reduction in RPE65 due to loss of MYO7A was slightly more pronounced in LA retinas than in dark-adapted (DA) retinas. This difference was due to a small increase in RPE65 levels that occurs in WT retinas in response to light, but not in shaker1 retinas. Retinas from mice that were DA for 16 h overnight, and then either kept in the dark or exposed to room lights for 2 h were compared. The 2 h exposure to light effected a 25% increase over DA RPE65 levels in WT retinas, but not in shaker1 retinas (Fig. 2C and D).

Degradation of RPE65

We tested whether the reduced levels of RPE65 in the shaker1 retina might be linked to increased protein degradation. The rate of loss of RPE65 was determined by treating eyecups with cycloheximide (CHX) to inhibit additional protein synthesis, and then measuring the amount of RPE65 at intervals. The amount of RPE was found to decrease more quickly in shaker1 eyecups; after 8 h, it had dropped by 50%, whereas in heterozygous eyecups it has decreased by only 25% over the same period (Fig. 2E and F). A similar experiment was performed with 293T cells that stably expressed RPE65, LRAT and CRALBP (23). In these cells, transfection with GFP-MYO7A increased the half-life of RPE65 from 4 to 5.5 h. Together, these results indicate that increased degradation contributes to the lower amount of RPE65 in shaker1 retinas.

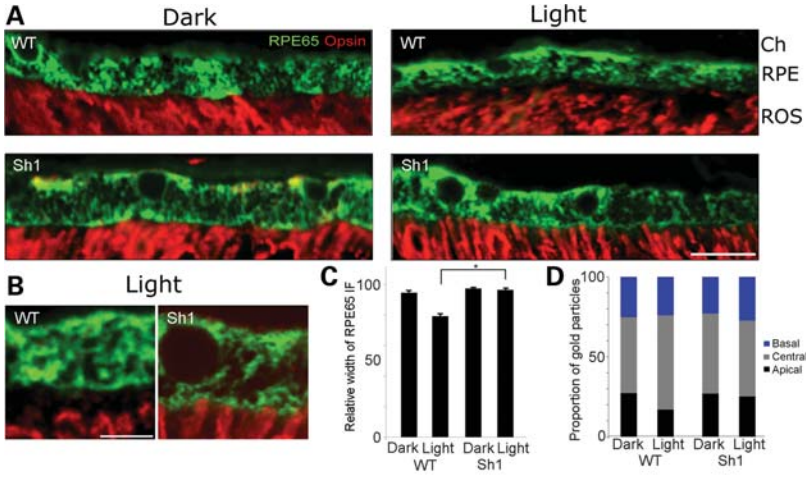

Figure 3. Subcellular localization of RPE65 is dependent on light and MYO7A. (**A**) Paraffin sections (5 μm) of WT and shaker1 (Sh1) retinas, either DA or LA, labeled with rhodopsin (red) and RPE65 (green) antibodies. RPE65 and opsin labeling are juxtaposed, except in the LA WT retina, where RPE65 is depleted from the apical RPE, and its labeling does not extend to the tips of the opsin-labeled outer segments. Ch, choroid; RPE, retinal pigment epithelium; ROS, rod outer segments. Scale bar = 15 μm. (**B**) Higher magnification of sections labeled in the same manner as those in *A*, comparing LA WT and shaker1 retinas. Scale bar = 2.5 μm. (**C**) Bar graph of measurements of the width of the immunofluorescence (IF) labeling in WT and shaker1 RPE sections, prepared and labeled as in (A) and (B). (**D**) Bar graph illustrating the distribution of RPE65 in the apical, central and basal regions of the RPE, in relation to the genotype and lighting conditions. The data were obtained from gold particle counts following immunogold labeling and electron microscopy. Basal to apical sections of the RPE were divided into equal thirds, and the gold particles were counted in each region.

Subcellular localization of RPE65

RPE65 is an RPE-specific protein. We studied its distribution within the RPE by immunofluorescence and immunoelectron microscopy. First, we observed that the distribution of RPE65 differs between LA and DA retinas of WT mice. In the dark, RPE65 is distributed more extensively throughout the cell; its distribution extends to the tips of the outer segments. But upon exposure to light (~100 lux, 2 h), it becomes concentrated more in the central region, so that a space is evident between the immunofluorescence labeling of the outer segments and that of RPE65 (Fig. 3A, upper panels). This difference occurs in mice containing either of the two RPE65 alleles (Leu450 or Met450) tested. It can also be observed by immunoelectron microscopy (Supplementary Material, Fig. S3).

Secondly, we observed that the distribution of RPE65 in shaker1 RPE differs from that in the WT. In particular, the protein does not undergo the same redistribution upon exposure to light. RPE65 extends to the level of the tips of the outer segments in both LA and DA shaker1 retinas. This distribution is comparable with that in DA WT retinas (Fig. 3A–C). The same observation was made with mice possessing a different mutation of *Myo7a*. *Polka* mice are not null for MYO7A, but express a mutant form of the protein that is truncated at its C-terminus. Like shaker1 mice, these mice have defects in cochlear hair cell development, and the melanosomes in their RPE are mislocalized (28). Supplementary Material, Figure S2 shows the distribution of RPE65 in LA WT and *polka* mutant RPE. In the WT RPE, RPE65 appears more concentrated in the central region of the RPE than in the mutant RPE, where more RPE65 labeling is evident in the apical RPE, below the cell nuclei.

Quantitative immunoelectron microscopy showed that the relative amount of RPE65 was increased somewhat in the central third of the RPE, following light exposure of WT retinas. No such increase in RPE65 was observed in the shaker1 RPE (Fig. 3D; Supplementary Material, Fig. S3). While the division of the RPE into three equal regions did not correspond to any given subcellular structures, and therefore may underestimate the effect, these observations were nevertheless consistent with the immunofluorescence data.

Together, our results on the subcellular localization of RPE65 show that there is a light-dependent change in the distribution of the protein, and that this phenomenon is abolished in the absence of MYO7A function.

Recovery after photobleach

Because the shaker1 RPE showed compromised RPE65 levels and distribution, we tested whether these effects were sufficient to manifest defects in retinoid levels and the retinal photoresponse after a photobleach. Experiments were performed with shaker1 mice and littermate controls on a 129 Sv background (homozygous for Leu450 RPE65), that were exposed to a ~50% photobleach, and then placed in the dark.

After 5 min in the dark, retinoid levels were similar between WT and shaker1 RPE, except the level of all-*trans*-retinyl palmitate, the RPE65 isomerase substrate. All-*trans*-retinyl ester levels were 54% higher in shaker1 RPE than in WT RPE ($P < 0.03$), suggesting less RPE65 activity (Fig. 4). In heterozygous (+/*sh1*) RPE, the mean level of all-*trans*-retinyl palmitate was 22% more than that in WT RPE, although statistical analysis of the data indicated no significant difference ($P > 0.07$).

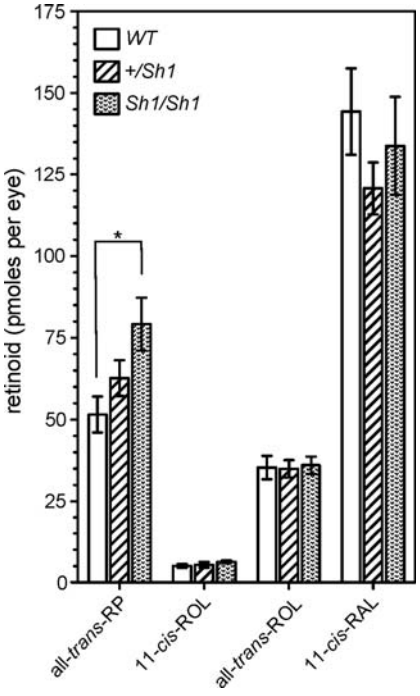

Figure 4. Measurements of retinoid levels during dark recovery following a photobleach. Levels of all-*trans*-retinyl palmitate (RP), 11-*cis*-retinol (ROL), all-*trans*-retinol and 11-*cis*-retinaldehyde (RAL) in eyecups of shaker1, +/*sh1* and WTmice, after 5 min in the dark following a 50–60% photobleach. All mice were homozygous for RPE65 Leu450. $^{*}P < 0.01$.

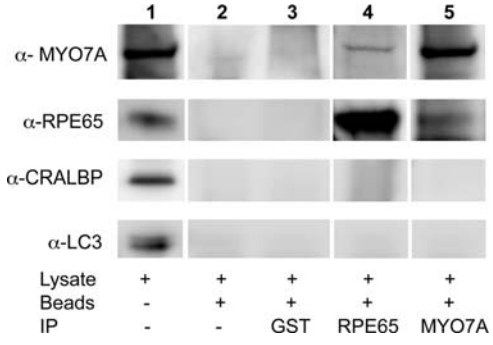

Figure 5. Immunoprecipitation of MYO7A with RPE65 antibody, and RPE65 with MYO7A antibody. Lane 1 shows immunolabeling of a western blot of the retinal lysate with MYO7A, RPE65, CRALBP and LC3 (microtubule-associated protein 1A/1B-light chain 3) antibodies. Lanes 2–5 show labeling of proteins associated with the protein A beads, following western blotting and using the same antibodies. GST antibody was used as a test for non-specific interactions (lane 3), and lack of antibody was used as a control for non-specific association with protein A beads (lane 2). Small amounts of MYO7A (lane 4) and RPE65 (lane 5) seem to associate directly or indirectly with the other protein, whereas two control proteins, CRALBP and LC3, do not.

The ERG was used to monitor photoreceptor activation (a-wave), and recovery of activation after light exposure. The waveforms of DA ERGs from shaker1 and +/*sh1* mice were indistinguishable (Supplementary Material, Fig. S4, inset). A light exposure was then used to examine the kinetics of recovery of photoreceptor function after a photobleach (~50%). The measured mean function describing the time course of recovery of the a-wave amplitude (expressed as a fraction of the DA amplitude) was slightly slower in shaker1 compared with +/*sh1* mice, but statistical analysis indicated no significant difference between the two functions (Supplementary Material, Fig. S4). At 50 min after the bleach, a-wave amplitude had reached levels of recovery in shaker1 ($38 \pm 21\%$ of the DA amplitude) and +/*sh1* ($51 \pm 17\%$) mice that were not significantly different ($P = 0.38$). Comparable results were obtained using the ERG b-wave to examine recovery. At 50 min after the bleach, recovery of the b-wave amplitude was $34 \pm 11\%$ in shaker1 and $41 \pm 14\%$ in +/*sh1* mice ($P = 0.15$).

Co-immunoprecipitation of MYO7A and RPE65

To test for a possible direct or indirect link between MYO7A and RPE65, we performed co-immunoprecipitation experiments on WT RPE. Small, but reproducible amounts of MYO7A and RPE65 were co-immunoprecipitated from RPE cell lysate with antibodies against the other protein, suggesting an interaction between the two proteins (Fig. 5). Neither protein was precipitated when a GST antibody (non-specific control) or beads alone were used, indicating the specificity of the MYO7A–RPE65 interaction. In addition, several other proteins, such as CRALBP and the microtubule-associated protein, LC3, did not associate with either precipitate. This result suggests that the RPE contains a complex that includes both MYO7A and RPE65, and which may be related to the MYO7A-dependent translocation of RPE65.

Colocalization of MYO7A and RPE65

MYO7A has been shown by immunolabeling of retinal sections to be distributed throughout the RPE, especially in the apical part of the cell body and in the apical processes (5,6,10,29,30). The distribution of RPE65 (cf. Fig. 3) overlaps with part of this described distribution for MYO7A. Here, we tested for colocalization of the two proteins by two different approaches. First, cells from the human RPE cell line, ARPE19, were co-transfected with *GFP-MYO7A* and *RFP-RPE65*, and confocal images were sequentially collected for each fluorophore from the same optical plane. Although the distributions of the two proteins differed, some overlap was evident, indicating partial colocalization (Fig. 6A–C). Secondly, we immunolabeled whole mounts of LA eyecups from 129 Sv mice, prepared as described previously (31), with antibodies against MYO7A and RPE65. Colocalization of the two proteins was evident primarily in the central regions of the RPE (Fig. 6D–G).

DISCUSSION

Based on the observation that shaker1 retinas are less susceptible to acute light damage, we investigated whether MYO7A was linked to the visual cycle. We show that retinas lacking MYO7A contain less of the visual cycle enzyme, RPE65, due to increased degradation. Moreover, the enzyme that is present fails to undergo light-dependent translocation, and the total isomerase activity is impaired. MYO7A and

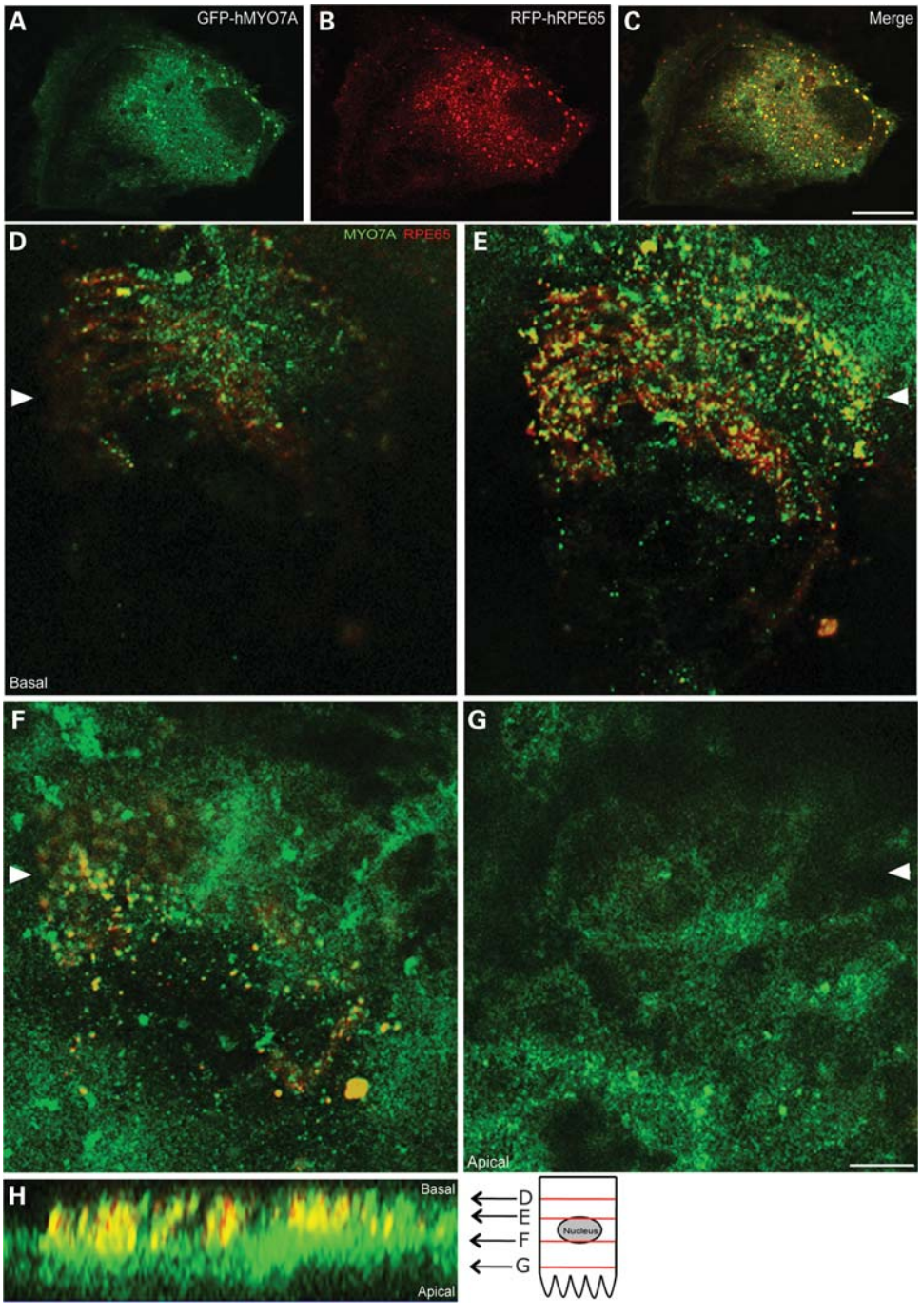

Figure 6. Fluorescence localization of MYO7A and RPE65. (**A**–**C**) Fluorescence images of an ARPE19 cell transfected with GFP-tagged human MYO7A (GFP-hMYO7A) (A) and RFP-tagged human RPE65 (RFP-hRPE65) (**B**). A merge of the green and red channels is shown in (C). Partial overlap in the distribution of the two proteins is evident. (**D**–**H**) Immunofluorescence labeling of MYO7A and RPE65 in a whole mount of a mouse eyecup. Confocal optical sections show different regions of the RPE, from basal (D) to apical (G). A reconstruction of the apical-basal axis, with relative locations of the optical sections (D–**G**), is shown (H). Arrowheads in (D)–(G) indicate the region corresponding to the apical–basal reconstruction. Scale bars = 5 μm.

RPE65 appear to be associated with each other, suggesting that MYO7A functions in the localization of the visual cycle enzyme.

Resistance to light damage, similar to that observed in shaker1 mice in the present study, was initially reported in strains of albino mice (32) that were found later to carry a sequence variation in *Rpe65* (26,27). It has also been documented in *Rpe65* knockout mice (22). Protection has been attributed to slowness in rhodopsin regeneration due to reduced RPE65 isomerase activity (27,33,34). The observed resistance to acute light damage in retinas of shaker1 mice, homozygous for the Leu450 allele of RPE65, is therefore consistent with a role for MYO7A in the visual cycle. Such a role is also indicated by reduced RPE65 levels, lack of RPE65

light-dependent translocation and increased retinyl ester accumulation in the shaker1 RPE, together with the association of MYO7A and RPE65 by co-immunoprecipitation and colocalization, all of which indicate that MYO7A function supports RPE65 isomerase activity.

Higher retinyl ester levels were measured in MYO7A-null eyecups during 5 min of dark recovery following a photobleach. Retinyl esters accumulate in two separate pools, in lipid droplets and in endoplasmic reticulum membranes (35). Here, we measured overall levels, making no distinction between these two pools; it is possible that the retinyl ester increase may have been due to only one of the pools, most likely the latter, which has been regarded as the 'isomerase pool' (35). We did not detect a difference in the levels of 11-*cis* retinaldehyde. However, this would have been unlikely, given that eyecups were used and most of this retinoid would have come from that remaining in the photoreceptor outer segments after the 50–60% photobleach. The amount of opsin in shaker1 retinas is similar to that in WT retinas (7). Previous studies, using similar experiments involving partial photobleaches, have also shown that retinyl ester levels are a more sensitive measure of RPE65 isomerase activity than 11-*cis*-retinal levels (36). The lack of significant difference in the ERG response during the dark recovery is consistent with the finding of no difference in 11-*cis* retinal levels, although, in this case, the comparison was made over a longer dark recovery period (50 min), and only between shaker1 mice and heterozygous (*+/sh1*) littermates (since WT congenic controls were unavailable for these experiments); *+/sh1* retinas appear to possess levels of RPE65 (Supplementary Material, Fig. S1) and retinyl esters (Fig. 5) that are between those found for shaker1 and WT. In conclusion, the >50% increase in all-*trans*-retinyl palmitate in shaker1 eyecups compared with WT eyecups, during short-term dark recovery after a photobleach, is a strong indication of impaired RPE65 activity in the absence of MYO7A.

RPE65 has been reported previously to be present in both the cytosolic and membrane fractions of RPE cells (37). It was suggested that palmitoylation of RPE65 provides a switch that allows for membrane association in a light-dependent manner (38); however, the association of RPE65 with membranes has since been shown to be independent of palmitoylation (39). Here, we provide evidence that a light exposure that follows dark adaptation results in an altered distribution of RPE65 within the RPE cell, with an increased concentration in the central region, where extensive smooth endoplasmic reticulum (SER) is present. RPE65 associates with retinol dehydrogenase 5 and retinal G protein-couple receptor (RGR) in a multi-protein complex on the SER (40,41). Significantly, the correct association of RPE65 with phospholipid membranes has recently been reported to be critical for its retinoid isomerization activity (41). This observation, coupled with the current finding of increased all-*trans* retinal ester levels in shaker1 RPE during dark recovery, suggests that MYO7A-dependent translocation of RPE65 to SER membrane in the central RPE helps regulate RPE65 activity in response to light. The lower level and shorter half-life of RPE65 in the absence of MYO7A suggests that mislocalization resulting from lack of translocation exposes RPE65 to faster proteolysis.

The dependence of this translocation of RPE65 upon MYO7A, and the association of MYO7A and RPE65 by partial co-immunoprecipitation and colocalization, is consistent with the participation of MYO7A in transporting RPE65, either directly or indirectly. An indirect means might involve MYO7A transport of SER membrane vesicles with which RPE65 is associated. Interestingly, class-5 unconventional myosins have been shown to associate with and move parts (vesicles or extensions) of ER in a variety of systems, such as squid axon (42), budding yeast (43) and dendrites of Purkinje cells (44–47). Moreover, MYO7A has already been shown to function like a MYO5 in the RPE with respect to another role: the mechanism by which it transports RPE melanosomes is comparable to how MYO5A transports melanosomes in melanocytes (10,48).

Usher syndrome involves progressive retinal degeneration. Mutant phenotypes in the retinas of *Myo7a*-mutant mice suggest possible underlying causes of degeneration in Usher 1B patients. A number of different such phenotypes have been described previously (7–10,49). Of these, the ones most likely to compromise photoreceptor and RPE cell health are an abnormally high level of opsin in the connecting cilium, slowed distal migration of the disk membranes and a delayed digestion of phagocytosed photoreceptor disk membranes (7,9). These phenotypes indicate deficiencies in the overall turnover of the outer segment disk membranes. It has been known for some time that complete disruption of any one of the stages of this turnover, such as disk morphogenesis in rds mice (50) or phagocytosis of the disk membrane by the RPE (51), causes retinal degeneration. In the present report, we describe an additional mutant phenotype that could contribute to retinal degeneration in Usher 1B. Loss-of-function mutations in the *RPE65* gene result in Leber congenital amaurosis, a recessively inherited blindness (52–54). Although impaired RPE65 function resulting from lack of MYO7A appears unlikely to be sufficient in itself to cause retinal degeneration in Usher 1B, it may contribute by adding further injury. Usher 1B may be the result of a combination of compromised, but not complete loss of function in several critical RPE-photoreceptor cell processes. In Usher 1B, one or more of these mutant phenotypes may be more severe than in mouse retinas, given that none of the mutant *Myo7a* mouse lines manifest retinal degeneration, including those with null alleles (55).

In conclusion, together our results indicate a role for MYO7A in the spatiotemporal regulation of the visual retinoid cycle. They suggest that MYO7A functions by mediating light-dependent translocation of RPE65. In addition, we propose that Usher 1B is likely to include defects in the visual cycle.

MATERIALS AND METHODS

Mice

All procedures conformed to institutional animal care and use authorizations, and with regulations established by the National Institutes of Health and the UK Home Office. Shaker1 mice, carrying the 4626SB allele, which is a Gln720X mutation in *Myo7a* (56), effecting a null mutation

(7), were used. This allele is referred to as simply shaker1 (*sh1)* in this report. Mice were genotyped as described previously (57). For the light damage study, mice were from an inbred colony on a mixed genetic background of ~50% CBA/Ca, ~50% BS, with some BALBc. They carried the WT allele at the albino locus, and the WT RPE65 (Leu450). For the other studies, mice were on either the C57BL/6HNsd (Harlan C57BL/6) genetic background, which contains the RPE65 Met450 variant, or backcrossed three generations from the C57BL6 stock on to the 129S2/SvPasCrl background (Charles River Laboratories) and selected for the WT RPE65 (Leu450).

Polka mice, from Dr Ulrich Mueller's lab, were reared under similar conditions. These mice carry a mutation (c.5742 + 5G>A) that affects splicing of the *Myo7a* transcript, resulting in MYO7A that lacks the C-terminal FERM domain (28). These mice had been crossed with 129S1/SvImJ mice, and were homozygous for the WT RPE65 (Leu450).

Mice were kept on a 12 h light/12 h dark cycle under 10–50 lux of fluorescent lighting during the light cycle. DA mice were handled using infrared converting binoculars. Except for the light damage experiment and photobleaching in the retinoid and ERG experiments (see below), light adaptation involved exposure to room fluorescent lighting of ~100 lux. For comparisons of dark and light adaptation, mice were DA for 16 h from late afternoon; LA mice were then exposed to 2 h of room lighting.

Light damage experiment

The pupils of each mouse were dilated 2 min before the onset of the light exposure, using topical atropine sulfate (600 μg/ml solution). The mice were placed in an animal cage lined with aluminum foil. The bottom of the cage had a dish of water, pellets of food and cut up pieces of fruit. The mice were exposed to 15 000 lux for 2 h. They were monitored throughout this period, and kept alert with their heads exposed. This was critical since the shaker1 mice are much more active than their controls; it was important to keep the controls as active. The cage temperature was continuously monitored with a digital thermometer and maintained within 3°C of room temperature. After exposure, the animals were returned to their vivarium, and maintained on the normal 12 h light/12 h dark cycle. Ten days after the high-light exposure, ERG measurements were obtained from the left eye of each animal, and both eyes were then enucleated and processed for light and electron microscopy.

Genotyping method for determining variant of RPE65

Rpe65 was analyzed by the PCR restriction fragment length polymorphism method. DNA was derived from mouse tails by standard procedures, and PCR amplified with the forward primer, 5′-GCATACGGACTTGGGTTGAATCAC-3′, and the reverse primer, 5′-GGTTGAGAAACAAAGATGGGT TCAG-3′. The resulting PCR product is 231 nt in length. The L450 variant contains an *Mwo*I site at nt 142–151 that is absent in the M450 variant. Digestion with *Mwo*I therefore resulted in two bands of ~142 and 89 bp for L450, and one band of 231 bp for M450.

Light and electron microscopy

Eyes were enucleated and posterior eyecups were fixed by immersion. The eyecups were fixed in 2% glutaraldehyde + 2% formaldehyde in 0.1 M cacodylate buffer, followed by secondary fixation in 1% OsO_4 and processing for embedment in Epon.

Photoreceptor cell density was determined from images of dorso-ventral semithin (0.7 μm) sections stained with toluidine blue. Regions that were spaced at 0.5 mm intervals from the optic nerve head were identified; the central retina corresponds approximately with the region that is 0.5 mm dorsal to the optic nerve head. In each region, at least three representative columns of photoreceptor cell nuclei were counted to determine the thickness of the nuclear layer in terms of the number of rows of nuclei.

Alternatively, eyecups were fixed in 0.25% glutaraldehyde + 4 formaldehyde in 0.1 M cacodylate buffer, pH 7.4 and processed for embedment in LR White. Ultrathin sections (70 nm) were subjected to saturated sodium periodate, blocked with 4% bovine serum albumin (BSA) in antibody buffer (TBS + 1% Tween-20) for 1 h at room temperature and incubated with RPE65 antibody in buffer overnight at 4°C. Sections were then washed and incubated with goat anti-rabbit IgG conjugated to 12 nm gold (Jackson Lab), and stained with uranyl acetate and lead citrate. Sections from RPE65 knockout mice were used as negative control. Immunolabeling density was determined by counting gold particles along the RPE. Random images were taken along the RPE layer, cells were divided into three equal regions (apical, central and basal) and gold particles were counted within each region. Statistical analyses for these and other experiments were performed using one-tail, Student *t*-tests.

Immunofluorescence analysis

For immunofluorescence microscopy, eyes were fixed in 4% formaldehyde in phosphate-buffered saline (PBS), and embedded in optimal cutting temperature compound (for cryosectioning) or paraffin. Sections (5 μm for paraffin, 8 μm for frozen) were rehydrated and blocked in 4% BSA in PBS. Autofluorescence was quenched with 50 mM ammonium chloride in PBS. After incubation with antibodies, sections were mounted using anti-fading mounting media containing 4′,6-diamidino-2-phenylindole (Fluorogel II, EMS, USA) and analyzed by confocal or epifluorescence microscopy. The primary antibodies were rabbit polyclonal (Pin5 from Dr Wenzel) or mouse monoclonal (from Dr Thompson) anti-RPE65 and mouse monoclonal anti-opsin (1D4 from Dr Molday). The secondary antibodies were Alexa 568 or Alexa 488 goat anti-rabbit or goat anti-mouse IgG (Molecular Probes, OR, USA).

Western blot analysis

Mouse eyecups were homogenized in 50 mM Tris, pH 7.4, 100 mM NaCl, 1 mM ethylenediaminetetraacetic acid (EDTA), 1 mM $MgCl_2$, 1 mM dithiothreitol (DTT), and complete protease inhibitor cocktail from Sigma. Equivalent protein concentrations were fractionated on a 4–12% Bis–Tris gel (Invitrogen) and transferred to polyvinylidene fluoride

(PVDF) membrane (Millipore). Membranes were blocked and then probed with the rabbit anti-RPE65 (1:1000), mouse anti-actin (JLA20) (1:1000), rabbit anti-RGR (from Dr Wenzel) (1:1000), rabbit anti-LRAT (from Dr Palczweski) (1:5000), rabbit anti-LC3 (microtubule-associated protein 1A/1B-light chain 3) (from Abgent) or rabbit anti-CRABLP (from Dr Saari) (1:1000), or washed, and incubated with horseradish peroxidase-conjugated anti-rabbit antibody (1:30 000, Sigma). Bound antibody was detected using the ECL Dura Western Blotting detection system (Thermo Scientific). The chemiluminescence signal detected was used to perform densitometry analysis in ImageJ, where the intensity was correlated with relative protein levels. Samples were analyzed in triplicate.

Half-life of RPE65

The rate of degradation of RPE65 was measured in the presence or absence of MYO7A, using two approaches: mouse eyecups, with neuroretinas removed, or a stable cell line, expressing RPE65, LRAT and CRALBP. For the first, retinas were gently peeled off the RPE, and the remaining eyecups were incubated with 50 μg/ml of CHX (Sigma), in dulbecco's modified eagle medium (DMEM) (Gibco) containing 10% fetal bovine serum (FBS) (Gibco) and 1× MEM (Gibco). Eyecups were collected at 0, 2, 4, 6 and 8 h after the addition of CHX. For the second approach, 293T-LRC cells that stably expressed RPE65, LRAT and CRALBP (23) were cultured in DMEM (Gibco), containing 10% FBS (Gibco) and 1× antibiotics (Gibco). Cells were plated at a density of 400 000 cells in six-well plates. The next day, half the wells were transfected with 1 μg of GFP-MYO7A complexed with Lipofectamine 2000 (Invitrogen), according to the manufacturer's instructions. After 48 h, cells were incubated with 50 μg/ml of CHX, and then collected at 0, 2, 4, 6, 8 and 10 h after the addition of the CHX. Collected eyecups and cells were lysed in lysis buffer (50 mM Tris, pH 7.4, 100 mM NaCl, 1 mM EDTA, 1 mM $MgCl_2$, 1 mM DTT and complete protease inhibitor cocktail from Sigma). Equivalent amounts of each sample were run on an 8% sodium dodecyl sulfate–polyacrylamide gel electrophoresis gel and transferred onto PVDF membranes. After immunolabeling, the amount of RPE65 was quantified by densitometry.

Retinoid measurements

Shaker1 mice and *Myo7a*$^{+/+}$ controls on a 129 Sv background (homozygous for Leu450 RPE65), at 6 weeks of age, were DA overnight, and anesthetized with an intraperitoneal injection of ketamine (4 mg/g body weight) and xylazine (0.8 mg/g body weight) in saline. Their pupils were then dilated with one drop of atropine sulfate (1%, w/v, in saline buffer) 30 min before exposure to 1000 lux in a Ganzfeld dome for 5 min. Mice were placed in the dark and were euthanized at intervals. Their eyes were enucleated, the anterior segment was removed and each resulting posterior eyecup was prepared and analyzed for retinoid content as described previously (35).

Electroretinography

Full-field ERGs were recorded as previously described (58,59). Mice were DA (>12 h), anesthetized and their pupils dilated (59). First, a DA photoresponse was elicited with a single bright (2.2 log scot-cd s m^{-2}) blue flash. After 2 min, a series of three white flashes (3.6 log scot-cd s m^{-2}) were presented in the dark at ∼5 s intervals, followed by a 2 min exposure to a white background (316 cd/m^2) light. This light exposure (∼50% photobleach) (60) completely suppressed the ERG a-wave. Recovery of the DA a-wave amplitude was assessed in the dark by presenting the bright blue stimulus every 10 min for a period of 50 min. Comparisons were made between congenic shaker1 (*sh1/sh1*) and heterozygous (*+/sh1*) mice, with the latter considered as controls (congenic WT mice were not available for this experiment). The mice (1–2 months old) were confirmed to carry the normal (Leu450) allele of RPE65. Student *t*-tests were performed on the data for each time point separately.

Immunoprecipitation

Mouse eyecups were homogenized in 300 mM NaCl, 50 mM Tris, pH 7, 1% CHAPS, 1 mM DTT and 1× complete protease inhibitor cocktail (Roche). Homogenates were clarified by centrifugation for 10 min at 5000*g* at 4°C. For each condition, 1 mg of lysate was diluted to a final volume of 500 μl with the homogenizing buffer. Samples were incubated with 2 μg of antibody (anti-RPE65, anti-Myo7a and anti-GST) overnight, with gentle rotation, at 4°C. Fifty microliters of protein A-sepharose beads (Amersham) were added to each tube and immune complexes were captured for 2 h at 4°C. Captured complexes were washed three times with lysis buffer, and boiled for 5 min at 100°C in sodium dodecyl sulfate gel loading buffer. Ten micrograms of lysate and immune complexes were separated and visualized by western blotting as described above.

Plasmids

N-terminal-tagged RFP-hRPE65 was generated using standard cloning strategies. Briefly, human RPE65 cDNA was amplified from clone 30915627 (Open Biosystems, USA), and ligated into the *Xho*I and *Kpn*I restriction sites of pENTRmRFP (from Dr Ramalho). The construct was confirmed by PCR colony screening, digestion of colonies and by sequencing.

Cotransfection of tagged MYO7A and RPE65

ARPE19 cells, a cell line derived from human RPE cells, were grown on glass cover slips. They were transfected with pEGFPC2-h*MYO7A* and pENTRmRFP-h*RPE65*, using complexes formed with Lipofectamine2000 (Invitrogen). Sixteen hours after transfection, cells were washed with PBS, fixed with 4% (w/v) paraformaldehyde prepared in PBS for 15 min. After washing, and incubation for 10 min with 50 mM NH_4Cl in PBS, cells were mounted with Fluoro-Gel (Electron Microscopy Sciences). They were visualized using a confocal microscope, and images representing single sections in the *z*-axis were obtained.

SUPPLEMENTARY MATERIAL

Supplementary Material is available at *HMG* online.

ACKNOWLEDGMENTS

We gratefully acknowledge Gabriel Travis for helpful discussions and providing the 293T cells stably-expressing RPE65, LRAT and CRALBP, Nathan Mata for discussions and help with preliminary experiments on retinoid measurements, Junko Kitamoto and Monalisa Mishra (Williams lab) for assistance in performing the research, Ulrich Mueller for the *polka* mice, John Ambrose (Steel lab) for genotyping, Andreas Wenzel for RPE65 and RGR antibodies, Debra Thompson for an RPE65 monoclonal antibody, Robert Molday for the opsin 1D4 antibody, Krzysztof Palczweski for the LRAT antibody, Jack Saari for the CRALBP antibody, Jose Ramalho for the pENTRmRFP vector and Michael Danciger for advice and help in breeding mice.

Conflict of Interest statement. None declared.

FUNDING

This work was supported by grants from the National Institutes of Health (grant numbers EY07042, EY00331, EY13203); Macula Vision Research Foundation; the Wellcome Trust (grant number 077189) and the Medical Research Council (UK). D.S.W. is a Jules and Doris Stein Research to Prevent Blindness Professor. Funding to pay the Open Access publication charges for this article was provided by the Wellcome Trust.

REFERENCES

1. Weil, D., Blanchard, S., Kaplan, J., Guilford, P., Gibson, F., Walsh, J., Mburu, P., Varela, A., Levilliers, J., Weston, M.D. *et al.* (1995) Defective myosin VIIA gene responsible for Usher syndrome type 1B. *Nature*, **374**, 60–61.
2. Gibson, F., Walsh, J., Mburu, P., Varela, A., Brown, K.A., Antonio, M., Beisel, K.W., Steel, K.P. and Brown, S.D.M. (1995) A type VII myosin encoded by mouse deafness gene shaker-1. *Nature*, **374**, 62–64.
3. Udovichenko, I.P., Gibbs, D. and Williams, D.S. (2002) Actin-based motor properties of native myosin VIIa. *J. Cell Sci.*, **115**, 445–450.
4. Inoue, A. and Ikebe, M. (2003) Characterization of the motor activity of mammalian myosin VIIA. *J. Biol. Chem.*, **278**, 5478–5487.
5. Hasson, T., Heintzelman, M.B., Santos-Sacchi, J., Corey, D.P. and Mooseker, M.S. (1995) Expression in cochlea and retina of myosin VIIa, the gene product defective in Usher syndrome type 1B. *Proc. Natl Acad. Sci. USA*, **92**, 9815–9819.
6. Liu, X., Vansant, G., Udovichenko, I.P., Wolfrum, U. and Williams, D.S. (1997) Myosin VIIa, the product of the Usher 1B syndrome gene, is concentrated in the connecting cilia of photoreceptor cells. *Cell Motil. Cytoskel.*, **37**, 240–252.
7. Liu, X., Udovichenko, I.P., Brown, S.D.M., Steel, K.P. and Williams, D.S. (1999) Myosin VIIa participates in opsin transport through the photoreceptor cilium. *J. Neurosci.*, **19**, 6267–6274.
8. Liu, X., Ondek, B. and Williams, D.S. (1998) Mutant myosin VIIa causes defective melanosome distribution in the RPE of shaker-1 mice. *Nat. Genet.*, **19**, 117–118.
9. Gibbs, D., Kitamoto, J. and Williams, D.S. (2003) Abnormal phagocytosis by retinal pigmented epithelium that lacks myosin VIIa, the Usher syndrome 1B protein. *Proc. Natl Acad. Sci. USA*, **100**, 6481–6486.
10. Gibbs, D., Azarian, S.M., Lillo, C., Kitamoto, J., Klomp, A.E., Steel, K.P., Libby, R.T. and Williams, D.S. (2004) Role of myosin VIIa and Rab27a in the motility and localization of RPE melanosomes. *J. Cell Sci.*, **117**, 6473–6483.
11. Williams, D.S. (2008) Usher syndrome: animal models, retinal function of Usher proteins, and prospects for gene therapy. *Vision Res.*, **48**, 433–441.
12. Noell, W.K., Walker, V.S., Kang, B.S. and Berman, S. (1966) Retinal damage by light in rats. *Invest. Ophthalmol.*, **5**, 450–473.
13. Sanyal, S. and Hawkins, R.K. (1986) Development and degeneration of retina in rds mutant mice: effects of light on the rate of degeneration in albino and pigmented homozygous and heterozygous mutant and normal mice. *Vision Res.*, **26**, 1177–1185.
14. Chen, J., Simon, M.I., Matthes, M.T., Yasumura, D. and LaVail, M.M. (1999) Increased susceptibility to light damage in an arrestin knockout mouse model of Oguchi disease (stationary night blindness). *Invest. Ophthalmol. Vis. Sci.*, **40**, 2978–2982.
15. Chen, C.K., Burns, M.E., Spencer, M., Niemi, G.A., Chen, J., Hurley, J.B., Baylor, D.A. and Simon, M.I. (1999) Abnormal photoresponses and light-induced apoptosis in rods lacking rhodopsin kinase. *Proc. Natl Acad. Sci. USA*, **96**, 3718–3722.
16. LaVail, M.M., Gorrin, G.M., Yasumura, D. and Matthes, M.T. (1999) Increased susceptibility to constant light in nr and pcd mice with inherited retinal degenerations. *Invest. Ophthalmol. Vis. Sci.*, **40**, 1020–1024.
17. Organisciak, D.T., Li, M., Darrow, R.M. and Farber, D.B. (1999) Photoreceptor cell damage by light in young Royal College of Surgeons rats. *Curr. Eye Res.*, **19**, 188–196.
18. Wald, G. and Brown, P.K. (1956) Synthesis and bleaching of rhodopsin. *Nature*, **177**, 174–176.
19. Bernstein, P.S., Law, W.C. and Rando, R.R. (1987) Isomerization of all-trans-retinoids to 11-cis-retinoids in vitro. *Proc. Natl Acad. Sci. USA*, **84**, 1849–1853.
20. Saari, J.C. (2000) Biochemistry of visual pigment regeneration: the Friedenwald lecture. *Invest. Ophthalmol. Vis. Sci.*, **41**, 337–348.
21. Travis, G.H., Golczak, M., Moise, A.R. and Palczewski, K. (2007) Diseases caused by defects in the visual cycle: retinoids as potential therapeutic agents. *Annu. Rev. Pharmacol. Toxicol.*, **47**, 469–512.
22. Grimm, C., Wenzel, A., Hafezi, F., Yu, S., Redmond, T.M. and Reme, C.E. (2000) Protection of Rpe65-deficient mice identifies rhodopsin as a mediator of light-induced retinal degeneration. *Nat. Genet.*, **25**, 63–66.
23. Jin, M., Li, S., Moghrabi, W.N., Sun, H. and Travis, G.H. (2005) Rpe65 is the retinoid isomerase in bovine retinal pigment epithelium. *Cell*, **122**, 449–459.
24. Moiseyev, G., Chen, Y., Takahashi, Y., Wu, B.X. and Ma, J.X. (2005) RPE65 is the isomerohydrolase in the retinoid visual cycle. *Proc. Natl Acad. Sci. USA*, **102**, 12413–12418.
25. Redmond, T.M., Poliakov, E., Yu, S., Tsai, J.Y., Lu, Z. and Gentleman, S. (2005) Mutation of key residues of RPE65 abolishes its enzymatic role as isomerohydrolase in the visual cycle. *Proc. Natl Acad. Sci. USA*, **102**, 13658–13663.
26. Danciger, M., Matthes, M.T., Yasamura, D., Akhmedov, N.B., Rickabaugh, T., Gentleman, S., Redmond, T.M., La Vail, M.M. and Farber, D.B. (2000) A QTL on distal chromosome 3 that influences the severity of light-induced damage to mouse photoreceptors. *Mamm. Genome*, **11**, 422–427.
27. Wenzel, A., Reme, C.E., Williams, T.P., Hafezi, F. and Grimm, C. (2001) The Rpe65 Leu450Met variation increases retinal resistance against light-induced degeneration by slowing rhodopsin regeneration. *J. Neurosci.*, **21**, 53–58.
28. Schwander, M., Lopes, V., Sczaniecka, A., Gibbs, D., Lillo, C., Delano, D., Tarantino, L.M., Wiltshire, T., Williams, D.S. and Muller, U. (2009) A novel allele of myosin VIIa reveals a critical function for the C-terminal FERM domain for melanosome transport in retinal pigment epithelial cells. *J. Neurosci.*, **29**, 15810–15818.
29. El-Amraoui, A., Sahly, I., Picaud, S., Sahel, J., Abitbol, M. and Petit, C. (1996) Human Usher 1B/mouse shaker-1: the retinal phenotype discrepancy explained by the presence/absence of myosin VIIA in the photoreceptor cells. *Hum. Mol. Genet.*, **5**, 1171–1178.
30. Gibbs, D. and Williams, D.S. (2004) Usher 1 protein complexes in the retina. *Invest. Ophthalmol. Vis. Sci.*, **45**, e-letter (26 May).
31. Gibbs, D., Diemer, T., Khanobdee, K., Hu, J., Bok, D. and Williams, D.S. (2010) Function of MYO7A in the human RPE and the validity of shaker1 mice as a model for Usher syndrome 1B. *Invest. Ophthalmol. Vis. Sci.*, **51**, 1130–1135.

32. LaVail, M.M., Gorrin, G.M., Repaci, M.A., Thomas, L.A. and Ginsberg, H.M. (1987) Genetic regulation of light damage to photoreceptors. *Invest. Ophthalmol. Vis. Sci.*, **28**, 1043–1048.
33. Nusinowitz, S., Nguyen, L., Radu, R., Kashani, Z., Farber, D. and Danciger, M. (2003) Electroretinographic evidence for altered phototransduction gain and slowed recovery from photobleaches in albino mice with a MET450 variant in RPE65. *Exp. Eye Res.*, **77**, 627–638.
34. Lyubarsky, A.L., Savchenko, A.B., Morocco, S.B., Daniele, L.L., Redmond, T.M. and Pugh, E.N. Jr (2005) Mole quantity of RPE65 and its productivity in the generation of 11-cis-retinal from retinyl esters in the living mouse eye. *Biochemistry*, **44**, 9880–9888.
35. Radu, R.A., Hu, J., Peng, J., Bok, D., Mata, N.L. and Travis, G.H. (2008) Retinal pigment epithelium-retinal G protein receptor-opsin mediates light-dependent translocation of all-trans-retinyl esters for synthesis of visual chromophore in retinal pigment epithelial cells. *J. Biol. Chem.*, **283**, 19730–19738.
36. Wenzel, A., Oberhauser, V., Pugh, E.N. Jr, Lamb, T.D., Grimm, C., Samardzija, M., Fahl, E., Seeliger, M.W., Reme, C.E. and von Lintig, J. (2005) The retinal G protein-coupled receptor (RGR) enhances isomerohydrolase activity independent of light. *J. Biol. Chem.*, **280**, 29874–29884.
37. Ma, J., Zhang, J., Othersen, K.L., Moiseyev, G., Ablonczy, Z., Redmond, T.M., Chen, Y. and Crouch, R.K. (2001) Expression, purification, and MALDI analysis of RPE65. *Invest. Ophthalmol. Vis. Sci.*, **42**, 1429–1435.
38. Xue, L., Gollapalli, D.R., Maiti, P., Jahng, W.J. and Rando, R.R. (2004) A palmitoylation switch mechanism in the regulation of the visual cycle. *Cell*, **117**, 761–771.
39. Jin, M., Yuan, Q., Li, S. and Travis, G.H. (2007) Role of LRAT on the retinoid isomerase activity and membrane association of Rpe65. *J. Biol. Chem.*, **282**, 20915–20924.
40. Pandey, S., Blanks, J.C., Spee, C., Jiang, M. and Fong, H.K. (1994) Cytoplasmic retinal localization of an evolutionary homolog of the visual pigments. *Exp. Eye Res.*, **58**, 605–613.
41. Golczak, M., Kiser, P.D., Lodowski, D.T., Maeda, A. and Palczewski, K. (2010) Importance of membrane structural integrity for RPE65 retinoid isomerization activity. *J. Biol. Chem.*, **285**, 9667–9682.
42. Tabb, J.S., Molyneaux, B.J., Cohen, D.L., Kuznetsov, S.A. and Langford, G.M. (1998) Transport of ER vesicles on actin filaments in neurons by myosin V. *J. Cell Sci.*, **111**, 3221–3234.
43. Estrada, P., Kim, J., Coleman, J., Walker, L., Dunn, B., Takizawa, P., Novick, P. and Ferro-Novick, S. (2003) Myo4p and She3p are required for cortical ER inheritance in Saccharomyces cerevisiae. *J. Cell Biol.*, **163**, 1255–1266.
44. Dekker-Ohno, K., Hayasaka, S., Takagishi, Y., Oda, S., Wakasugi, N., Mikoshiba, K., Inouye, M. and Yamamura, H. (1996) Endoplasmic reticulum is missing in dendritic spines of Purkinje cells of the ataxic mutant rat. *Brain Res.*, **714**, 226–230.
45. Takagishi, Y., Oda, S., Hayasaka, S., Dekker-Ohno, K., Shikata, T., Inouye, M. and Yamamura, H. (1996) The dilute-lethal (dl) gene attacks a Ca2+ store in the dendritic spine of Purkinje cells in mice. *Neurosci. Lett.*, **215**, 169–172.
46. Wagner, W. and Hammer, J.A. 3rd (2003) Myosin V and the endoplasmic reticulum: the connection grows. *J. Cell Biol.*, **163**, 1193–1196.
47. Wagner, W., Brenowitz, S.D. and Hammer, J.A. 3rd (2011) Myosin-Va transports the endoplasmic reticulum into the dendritic spines of Purkinje neurons. *Nat. Cell Biol.*, **13**, 40–48.
48. El-Amraoui, A., Schonn, J.S., Kussel-Andermann, P., Blanchard, S., Desnos, C., Henry, J.P., Wolfrum, U., Darchen, F. and Petit, C. (2002) MyRIP, a novel Rab effector, enables myosin VIIa recruitment to retinal melanosomes. *EMBO Rep.*, **3**, 463–470.
49. Libby, R.T. and Steel, K.P. (2001) Electroretinographic anomalies in mice with mutations in Myo7a, the gene involved in human Usher syndrome type 1B. *Invest. Ophthalmol. Vis. Sci.*, **42**, 770–778.
50. Jansen, H.G. and Sanyal, S. (1984) Development and degeneration of retina in rds mutant mice: electron microscopy. *J. Comp. Neurol.*, **224**, 71–84.
51. Bok, D. and Hall, M.O. (1971) The role of the pigment epithelium in the etiology of inherited retinal dystrophy in the rat. *J. Cell Biol.*, **49**, 664–682.
52. Thompson, D.A., Gyurus, P., Fleischer, L.L., Bingham, E.L., McHenry, C.L., Apfelstedt-Sylla, E., Zrenner, E., Lorenz, B., Richards, J.E., Jacobson, S.G. *et al.* (2000) Genetics and phenotypes of RPE65 mutations in inherited retinal degeneration. *Invest. Ophthalmol. Vis. Sci.*, **41**, 4293–4299.
53. Jacobson, S.G., Aleman, T.S., Cideciyan, A.V., Roman, A.J., Sumaroka, A., Windsor, E.A., Schwartz, S.B., Heon, E. and Stone, E.M. (2009) Defining the residual vision in leber congenital amaurosis caused by RPE65 mutations. *Invest. Ophthalmol. Vis. Sci.*, **50**, 2368–2375.
54. Philp, A.R., Jin, M., Li, S., Schindler, E.I., Iannaccone, A., Lam, B.L., Weleber, R.G., Fishman, G.A., Jacobson, S.G., Mullins, R.F. *et al.* (2009) Predicting the pathogenicity of RPE65 mutations. *Hum. Mutat.*, **30**, 1183–1188.
55. Lillo, C., Kitamoto, J., Liu, X., Quint, E., Steel, K.P. and Williams, D.S. (2003) Mouse models for Usher syndrome 1B. *Adv. Exp. Med. Biol.*, **533**, 143–150.
56. Mburu, P., Liu, X.Z., Walsh, J., Saw, D. Jr, Cope, M.J., Gibson, F., Kendrick-Jones, J., Steel, K.P. and Brown, S.D. (1997) Mutation analysis of the mouse myosin VIIA deafness gene. *Genes Funct.*, **1**, 191–203.
57. Holme, R.H. and Steel, K.P. (2002) Stereocilia defects in waltzer (Cdh23), shaker1 (Myo7a) and double waltzer/shaker1 mutant mice. *Hear. Res.*, **169**, 13–23.
58. Aleman, T.S., LaVail, M.M., Montemayor, R., Ying, G., Maguire, M.M., Laties, A.M., Jacobson, S.G. and Cideciyan, A.V. (2001) Augmented rod bipolar cell function in partial receptor loss: an ERG study in P23H rhodopsin transgenic and aging normal rats. *Vision Res.*, **41**, 2779–2797.
59. Roman, A.J., Boye, S.L., Aleman, T.S., Pang, J.J., McDowell, J.H., Boye, S.E., Cideciyan, A.V., Jacobson, S.G. and Hauswirth, W.W. (2007) Electroretinographic analyses of Rpe65-mutant rd12 mice: developing an in vivo bioassay for human gene therapy trials of Leber congenital amaurosis. *Mol. Vis.*, **13**, 1701–1710.
60. Lyubarsky, A.L., Daniele, L.L. and Pugh, E.N. Jr (2004) From candelas to photoisomerizations in the mouse eye by rhodopsin bleaching in situ and the light-rearing dependence of the major components of the mouse ERG. *Vision Res.*, **44**, 3235–3251.